

Provided for non-commercial research and education use.  
Not for reproduction, distribution or commercial use.



This article appeared in a journal published by Elsevier. The attached copy is furnished to the author for internal non-commercial research and education use, including for instruction at the authors institution and sharing with colleagues.

Other uses, including reproduction and distribution, or selling or licensing copies, or posting to personal, institutional or third party websites are prohibited.

In most cases authors are permitted to post their version of the article (e.g. in Word or Tex form) to their personal website or institutional repository. Authors requiring further information regarding Elsevier's archiving and manuscript policies are encouraged to visit:

<http://www.elsevier.com/copyright>



Contents lists available at SciVerse ScienceDirect

## Journal of Asian Earth Sciences

journal homepage: [www.elsevier.com/locate/jseas](http://www.elsevier.com/locate/jseas)

# Clay mineralogy and geochemistry investigations in the host rocks of the Chelungpu fault, Taiwan: Implication for faulting mechanism

Li-Wei Kuo<sup>a,\*</sup>, Sheng-Rong Song<sup>a</sup>, En-Chao Yeh<sup>b</sup>, Huei-Fen Chen<sup>c</sup>, Jialiang Si<sup>d</sup>

<sup>a</sup> Department of Geosciences, National Taiwan University, Taiwan

<sup>b</sup> Department of Earth Sciences, National Taiwan Normal University, Taiwan

<sup>c</sup> Institute of Applied Geosciences, National Taiwan Ocean University, Taiwan

<sup>d</sup> Institute of Geology, Chinese Academy of Geological Sciences, China

## ARTICLE INFO

### Article history:

Received 14 December 2011

Received in revised form 10 July 2012

Accepted 16 July 2012

Available online 4 August 2012

### Keywords:

Clay minerals

Major elements

Chemical weathering

The Chelungpu fault

## ABSTRACT

The Chelungpu fault, with northward propagating ruptures, was ruptured as a result of the  $M_w$  7.6 earthquake which struck Central Taiwan on 21st September 1999. To understand the consequences of clays in fault gouges, we examined the clay mineralogy and major element geochemistry of the “host rocks” of the Chelungpu fault from four outcrops, shallow boreholes at Fengyuan (455.3 m in depth), Nantou (211.9 m in depth), and a deep borehole of the Taiwan Chelungpu fault Drilling Project (2003 m in depth). Results revealed different degrees of chemical weathering, the intensity, as documented by differences in the smectite content, could be further understood through the relative clay percentage of smectite, illite chemistry index, and illite crystallinity. These mineralogical proxies combined with the chemical index of alteration (CIA) and the intensity of chemical weathering indicate that the degree of chemical weathering is a function of depth, i.e., the most severe on the surface and the mildest in the TCDP samples. The mineralogical and geochemical data obtained in this study also suggest that chemical weathering, rather than leaching, seems to be the main driving force for the phase changes of clays. The amount of smectite produced by chemical weathering varies with depth, and it suggests that the previous idea of weak-fault caused by the presence of smectite in the fault zone will be risky without considering weathering processes. The observations of clay mineralogy and major element geochemistry in this study indicate that the presence of smectite in the outcrops may not play a significant role during faulting, and suggest that fault-weakening as a result of the presence of smectite cannot be applied to the Chelungpu fault.

© 2012 Elsevier Ltd. All rights reserved.

## 1. Introduction

Clay gouges in faulted sedimentary rock are often described as shales smear forming through the mechanical incorporation of protolith rocks into a fault zone (Yielding et al., 1997; Jones and Hillis, 2003). Moreover, several studies have described fault gouges from a chemical point of view through characterization of fault-related clay mineralization for clay gouge formation (Vrolijk and van der Pluijm, 1999; Solum et al., 2005). The factors controlling clay genesis and transformation such as fluid, heat, strain energy, and time are usually taken into account to investigate faulting behaviors (Whitney, 1990; Moore and Reynolds, 1997; Solum et al., 2005; Isaacs et al., 2007; Kuo et al., 2009, 2011). Thus, many studies of clays in fault zones show the implications for fault mechanics (Solum et al., 2003; Takahashi et al., 2007; Brantut et al., 2008; Boutareaud et al., 2010; Di Toro et al., 2011). Observations of nat-

ural faults and experimental results of fault gouges indicate that they are mechanically weaker than predicted from Byerlee's Law (Mount and Suppe, 1987; Zoback, 2000; Han et al., 2007; Mizoguchi et al., 2009; Di Toro et al., 2011; Lockner et al., 2011). Elevated fluid pressure and a corresponding reduction in effective stress is a possible cause of weakening a fault (Sibson, 1990, 2003; Rice, 1992; Faulkner and Rutter, 2001). On the other hand, no indication of elevated fluid pressure at San Andreas Fault Observatory at Depth (SAFOD) was found for fault weakening (Lockner et al., 2011). Generally speaking, changes in permeability along a fault zone depend on the extent of clay minerals growth and their mechanical incorporation in the fault core which may affect faulting mechanism (Wang, 1984; Rice, 1992). The behavior of clay minerals in a fault zone is obviously an important indicator for investigating the faulting mechanism. However, very few quantitative measurements of clay minerals in a fault zone have been made to evaluate the influence of the chemical weathering process (Solum et al., 2003). The faulting mechanism and/or fault-related processes for a fault might be incorrectly interpreted via discussing clay mineral assemblages caused by chemical weathering. Thus, instead of analyzing fault gouge and/or damaged rocks which have

\* Corresponding author. Address: No. 1, Sec. 4, Roosevelt Road, Taipei 10617, Taiwan. Fax: +886 2 23636095.

E-mail addresses: [liweikuo@ntu.edu.tw](mailto:liweikuo@ntu.edu.tw), [liweikuo@gmail.com](mailto:liweikuo@gmail.com) (L.-W. Kuo), [srsong@ntu.edu.tw](mailto:srsong@ntu.edu.tw) (S.-R. Song).

been influenced by physicochemical reactions during coseismic events and/or aseismic periods, in this study we collected the fresh and unweathered host rocks that contain original fabrics extracted from different areas and at different depth along the Chelungpu fault to explore the chemical weathering process.

The Chelungpu thrust fault is an active fault that ruptured on 21st September 1999 with  $M_w$  7.6 near the town of Chi-Chi of central Taiwan (Fig. 1). The Chi-Chi earthquake produced northward propagating ruptures with a ~90 km long north–south trending rupture surface (Ma et al., 2000; Chen et al., 2001; Lee et al., 2001). The coseismic slip and rupture velocity increased northward along the fault, which led to a much larger horizontal displacement (5–9 m) in the northern segment compared to that (2 m) in the southern part (Ma et al., 2000; Chen et al., 2001; Lee et al., 2001; Yue et al., 2005). Strong ground motion of high-frequency acceleration was found to decrease from south to north (Lin et al., 2001). This NS-trending thrust dipped eastward at about 30°, and was nearly pure thrust slip near the epicenter, and changed to oblique thrust with a strong left-lateral component during the Chi-Chi event (Chen et al., 2001).

After the Chi-Chi earthquake, we collected host rock samples surrounding the Chelungpu fault zones at Yichiang Bridge (site 1), Kungfu elementary school (site 2), Nantou Dapi (site 3), and Tungtou Bridge (site 4) (hereafter YCB, KF, NT, and TTB, respectively), from north to south, to explore the fault-related clay mineralization (Fig. 1). Besides, two shallow drillings across the Chelungpu fault were also carried out at Fengyuan (Fig. 1, shown as northern drill site; the depth of borehole is 455.3 m) and at Nantou (Fig. 1, shown as southern drill site; the depth of borehole is 211.9 m) to investigate the difference in seismic slip mechanisms between northern and southern fault segments (Tanaka et al., 2002). To obtain more advanced and comprehensive physical and chemical details of the Chelungpu fault zone, Taiwan Chelungpu fault Drilling Project (TCDP) was conducted in 2005. Two holes, namely Hole-A and

Hole-B, were drilled with side-track coring 6 km south of the Fengyuan site and 2 km east of the surface rupture of the Chelungpu fault (Fig. 1; the depth of borehole-A is 2003 m).

The presence of smectite has long been thought to be weakening material in fault (Byerlee, 1970; Wang, 1984; Rice, 1992). Thus, the assemblages of clay minerals from the sites mentioned above have been used to investigate the fault-related processes (Liao, 2003; Isaacs et al., 2007; Chen et al., 2007; Hirono et al., 2008; Kuo et al., 2009, 2011), and the reaction of smectite to illite is utilized to interpret the presumable faulting mechanisms and/or fault-related processes of the Chelungpu fault. These previous studies have concluded that the clays along the Chelungpu fault were related to the faulting processes (Liao, 2003; Chen et al., 2007; Isaacs et al., 2007). Liao (2003) analyzed samples from the shallow borehole of Fengyuan, and suggested that smectite in the gouges converts into a mixed layer of illite/smectite with heat produced by coseismic events. Chen et al. (2007) examined the samples from the shallow borehole of Nantou, and presented the data of major elements and clay mineral assemblages to demonstrate the acid fluid–rock interactions during coseismic events. Isaacs et al. (2007) analyzed materials from the surface of the fault outcrops, and suggested that smectite along the Chelungpu fault was formed by weathering, and might have been influenced by co-seismic fluid flow to activate the reaction of illite–smectite. Kuo et al. (2009) discovered that the smectite-rich black gouge devitrified from pseudotachylyte might be related to the 1999 Chi-Chi earthquake. Moreover, rock mechanics experiments with outcrop samples have also been attempted for investigating the faulting behavior (Lin et al., 2000). In summary, the presence of smectite in their samples provides a low friction for the Chelungpu fault and/or has been suggested to explain the weakening behavior and/or fault-related processes during coseismic events.

However, smectite is well known as a common weathering product at shallow depths (Pédro, 1981), and the presence of smectite

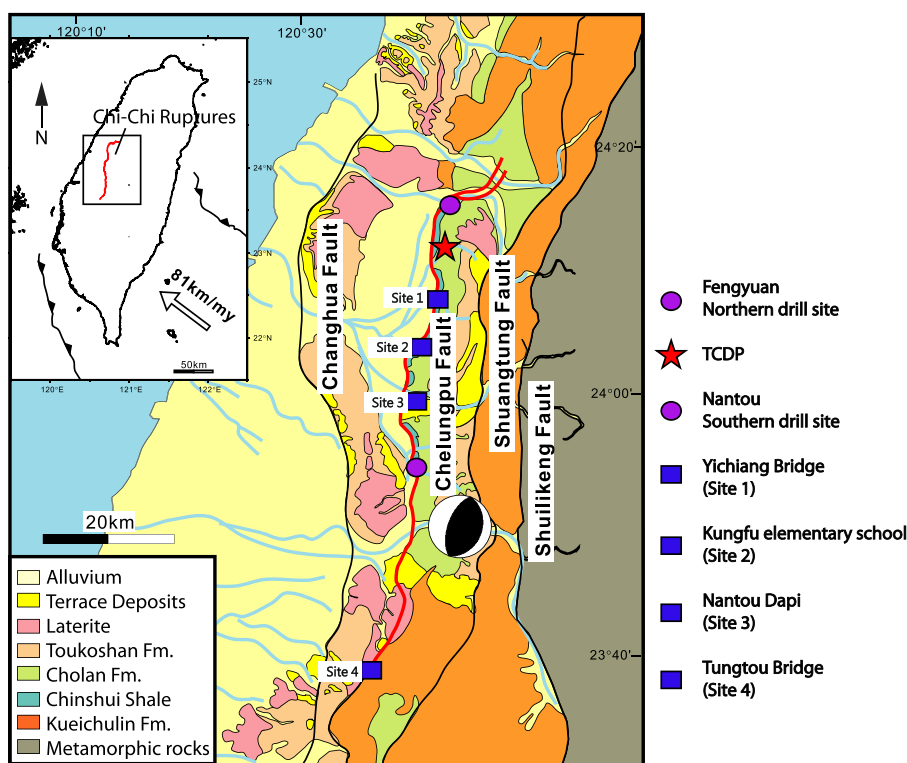


**Fig. 1.** Geological map of the central part of western Taiwan showing the distribution of formations and major faults. The four outcrops are shown as blue squares. The TCDP site is indicated by a red star. The two shallow boreholes of Fengyuan and Nantou are marked as purple circles. The focal mechanism of the Chi-Chi main shock is located at the hypocenter of the Chi-Chi earthquake. (For interpretation of the references to color in this figure legend, the reader is referred to the web version of this article.)

caused by chemical weathering should be considered while discussing fault-related process with the illite–smectite reaction (Solum et al., 2005). In this study, clay mineralogy and major element geochemistry were investigated for the first time on the host rocks from three formations (Cholan Formation, Chinshui shale, and Kueichulin formation) along the Chelungpu fault in order to evaluate the chemical weathering process. To obtain information on the degree of weathering, chemical index of alteration (CIA) was combined with clay mineralogical data (clay mineral composition, illite chemistry index, and illite crystallinity). The results from these investigations provide a qualitative description on weathering process and provide important insights before approaching real faulting mechanism and/or fault-related processes of the Chelungpu fault.

## 2. Geological setting and sampling

The Chelungpu thrust fault is part of the fold and thrust belt of the western Taiwan orogen that cuts shallow marine upper Miocene and Pliocene siltstones, shales, and sandstones of the Kueichulin (0.8–2 km thick shallow marine sandstones and shales), Chinshui (~300 m thick shales and siltstones), and Cholan Formations (1.5–2.5 km thick monotonous alternating sandstones and siltstones) (Fig. 1; Covey, 1984; Ho, 1988). The stratigraphic formations define the boundary between the western foothills and foreland basin (Chiu, 1971; Suppe, 1981; Heermance et al., 2003) (Fig. 1). The fault dips to the east at an angle of 52–60° in the northern segment and places siltstones of the Cholan, Chinshui and Kueichulin Formations on those of the Cholan Formation (Lee et al., 2001; Heermance et al., 2003). The Chelungpu fault flattens to the east with a dip of approximately of 25–35° in the southern segment (Kao and Chen, 2000; Heermance et al., 2003), and places siltstones of the Chinshui and Kueichulin Formations on Pleistocene Toukoshan gravels (Heermance, 2002; Tanaka et al., 2002). All samples collected in this study came from the Cholan Formation, the Chinshui Shale, and the Kueichulin Formation.

Four outcrops, namely YCB, KF, NT, and TTB, were investigated for field and chemical compositions after 1999 Chi-Chi earthquake (Fig. 2). Thirteen, ten, eleven, and eleven host rock samples were collected from YCB, KF, NT, and TTB, respectively. These samples belong to the Chinshui Shale at YCB, and KF, and from the Cholan Formation at NT, and from the Kueichulin Formation at TTB (Table 1). The host rocks collected from the outcrops were fresh and were almost unweathered. Moreover, the weathering rind of outcrop samples was removed before chemical analyses to display a large-scale geologic process instead of a cm-scale surface weathering reaction.

We also integrated our analyses with the literature data of clays and major elements of host rocks from both shallow and deep boreholes. The shallow borehole data (455.3 m deep) of the northern site at Fengyuan which drilled through the Chinshui and Kueichulin Formations are mainly derived from Liao (2003). The data from the southern site at Nantou (211.9 m deep) that deal with the Chinshui Shale are derived from Chen et al. (2007). One hundred data of host rocks of TCDP at Dakeng which were recovered from the Cholan, Chinshui, and Kueichulin Formations (600–2003 m) were extracted from Kuo et al. (2009) (Fig. 2).

## 3. Analytical methods

In our study, a PANalytical X'Pert PRO X-ray diffractometer was used under the conditions of filtered Cu K $\alpha$  (1.540 Å) radiation at 45 kV and 40 mA, 1.0° min<sup>-1</sup> scanning speed, and 5–40° of 2 $\theta$  interval. For identifying and quantifying clay minerals of the <2  $\mu$ m grain-size fraction, glass slides of oriented clay samples were made. All samples were disaggregated in distilled water by using an ultrasonic bath. After centrifugation, suspensions of <2  $\mu$ m fraction were deposited on glass slides. Two XRD runs were performed, following air-drying and ethylene-glycol solvation for 72 h to identify swelling clays (smectite and mixed layered clay minerals

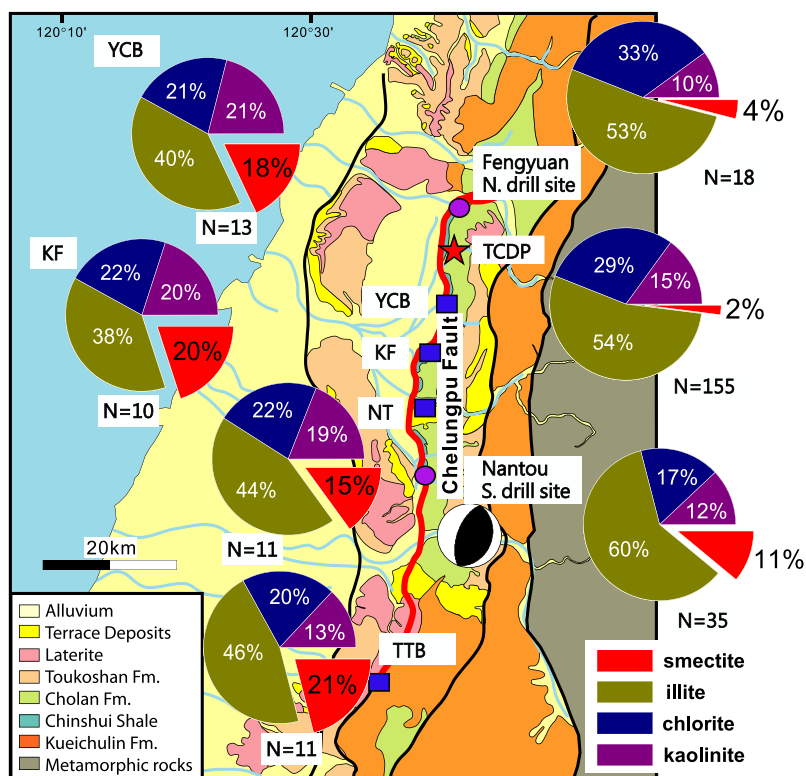


Fig. 2. Sample locations and distribution of average clay mineral assemblages in the four outcrops, the two shallow boreholes of Fengyuan and Nantou, and the deep borehole (TCDP). N is the number of host rock samples analyzed in the same location.

**Table 1**

Average clay mineral assemblages of various regions in outcrops, the Fengyuan northern drill site, TCDP, and the Nantou southern drill site. *N* is the number of host rock samples analyzed with XRF.

Sample	Sample (N)	Formation	Illite (%)	Smectite (%)	Chlorite (%)	Kaolinite (%)	Illite crystallinity ( $^{\circ}\Delta 2\theta$ )	Illite chemistry index	XRF (N)
YCB	13	Chinshui	40	18	21	21	0.33	0.65	3
KF	10	Chinshui	38	22	20	20	0.39	0.71	3
NT	11	Cholan	44	15	22	19	0.31	0.45	5
TTB	11	Kueichulin	46	21	20	13	0.35	0.41	5
Fengyuan	17	Chinshui	53	4	33	10	0.33	0.64	4
		Kueichulin							
Nantou	36	Chinshui	60	11	17	12	0.35	0.65	36
TCDP	100	Cholan	54	2	29	15	0.25	0.50	100
		Chinshui							
		Kueichulin							

such as illite/smectite and chlorite/smectite). Identification of clay minerals was made mainly according to the position of the (001) series of the basal reflections on the air-dried and glycolated XRD diagrams. In this study we utilize the most common approach for semi-quantitative analysis of clay minerals in powders, involving peak intensity ratios and mineral intensity factors (MIFs) (Kahle et al., 2002). This approach simplifies the general relationship between the integrated intensity of a diffraction peak area and the weight fraction of the mineral in a mixture. Peak areas of illite (10 Å), kaolinite (7 Å), and chlorite (14 Å) were divided based on their own reflection factors, which were calculated on the glycolated curve. Mixed-layer phases of chlorite/smectite 001/001 ( $x > 14.3$  Å) and illite/smectite 001/001 ( $x > 10$  Å) upon glycolation were determined (Biscaye, 1965; Fagel et al., 2003; Solum et al., 2003). Relative proportions of kaolinite and chlorite were determined on the basis of the ratio at the 3.57/3.54 Å peak area (Liu et al., 2007).

To compare the variation of chemical compositions in different samples, X-ray Fluorescence (XRF) was conducted in this study. The percentage of ten major and minor oxides, namely SiO<sub>2</sub>, Al<sub>2</sub>O<sub>3</sub>, Fe<sub>2</sub>O<sub>3</sub>, K<sub>2</sub>O, MnO, MgO, CaO, Na<sub>2</sub>O, TiO<sub>2</sub>, and P<sub>2</sub>O<sub>5</sub>, were determined by using a Rigaku RIX 2000 X-ray fluorescence at the Department of Geosciences, National Taiwan University. Analytical reproducibility for most oxides was less than 2% relative error, except for Na<sub>2</sub>O with an error of about 5% (Yang et al., 1996).

The illite chemistry index and illite crystallinity have been also calculated from the X-ray diffraction patterns after background subtraction. Illite chemistry index (Esquevin-indices) refers to the ratio of the 5–10 Å peak areas (Esquevin, 1969). Illite composition indicates the degree of weathering and can be used to trace the source of illites (e.g., Liu et al., 2007). Illite chemistry index vary between 0 and 1, and in general, ratios below indicate 0.5 represent Fe, Mg-rich unweathered illites reflecting physically eroded rocks whereas ratios above 0.5 indicate Al-rich illites that form under string hydrolysis (Esquevin, 1969; Gingele, 1996; Gingele et al., 2001; Wan et al., 2010). In the 1970s, illite crystallinity was developed to estimate the relative maturity or state of diagenesis of illite mixed-layer clay minerals in sedimentary rocks. Weaver (1960) introduced the concept of the Sharpness Ratio (Weaver index, WI) determining the ratio of the height of the 001 illite peak at 10 Å to the height at 10.5 Å. Later illite crystallinity obtained from the Full Width at Half Maximum (FWHM) of the 10 Å peak defined was introduced by Kübler (1964, 1967) (Kübler index, KI) and the unit of illite crystallinity is used to express as mm and  $^{\circ}\Delta 2\theta$  (e.g., Buchovecky and Lundberg, 1988; Dorsey et al., 1988). While fundamentally related, the WI and KI may vary due to the influence of hydroxyl Al-interlayered vermiculite or smectite on the width of the illite peak. After carefully check the glycolation and air-dried X-ray diffraction data, it suggests that there is no great difference between each other. Thus, in this study we utilize KI as determining the value of illite crystallinity and followed the procedure described by Kisch (1991) and use  $^{\circ}\Delta 2\theta$  as the unit for illite crystallinity.

## 4. Results

### 4.1. Clay minerals

Mixed-layer phases of clays in our samples were determined through the XRD data of air-dried and glycolated condition and it suggests that smectite-rich illite were dominant (Fig. 3). Here we follow the definition for the illite provided by Meunier and Velde (2004) and simply call smectite-rich illite mixed-layer as smectite hereafter. The four kinds of clay minerals found in the YCB, KF, NT and TTB outcrops are illite, smectite, chlorite and kaolinite (Fig. 2, left pie diagrams). The relative abundance of each mineral varies significantly in a given outcrop. Overall, illite is the most abundant phase among the four clay minerals, with an average abundance of 38–46%. Chlorite and kaolinite are roughly of equal abundance (~20%), and smectite is the least abundant clay mineral, with an average percentage ranging from 15% to 21% (Table 1). However, it should be pointed out that TTB has more smectite (~21%) than kaolinite (~13%).

In the northern shallow borehole of Fengyuan, illite, smectite, chlorite, and kaolinite were found (Fig. 2; on the right top; Liao, 2003). Similar to the four outcrops mentioned above, illite (41–82%) is the dominant clay mineral with an average of 52%; chlorite (10–46%) and kaolinite (2–15%) are less abundant with an average content of about 34% and 10%, respectively. Smectite (1–7%) has the lowest weight percent with an average content of 4% (Table 1).

In the TCDP case, illite, smectite, chlorite and kaolinite were recognized in one hundred host rock samples (Fig. 2; on the right middle; Kuo et al., 2009). The relative abundances of the four

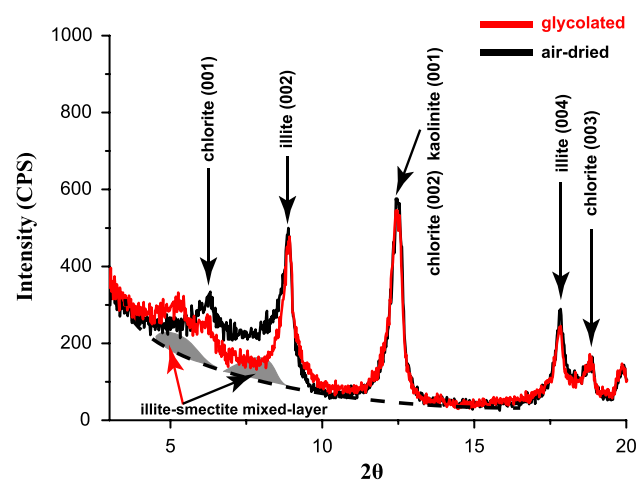


**Fig. 3.** X-ray diffraction patterns of the samples for identifying illite–smectite mixed-layer. Black and red lines are the results from air-dried and glycolated samples, respectively. Gray areas are the identified peak of smectite-rich illite. (For interpretation of the references to color in this figure legend, the reader is referred to the web version of this article.)

phases are similar to those found in the northern borehole samples, in the order of illite (37–81%), chlorite (12–41%), kaolinite (6–20%) and smectite (0–6%) (Table 1).

In the clay fraction of the southern shallow borehole of Nantou, illite, smectite, chlorite, and kaolinite were identified in 36 clay samples (Fig. 2; on the right bottom; Chen et al., 2007). Illite, chlorite, kaolinite and smectite have a relative percentage of 53–66%, 12–27%, 2–22% and 5–16%, respectively.

The XRD results of host rocks suggest that the mineral assemblages and similar abundance of clays are in good agreement with in the Cholan Formation, Chinshui Shale, and Kueichulin Formation except the presence of smectite.

#### 4.2. Major elements

Sixteen host rock samples from the four outcrops and one hundred host rock samples from the TCDP were analyzed by XRF for major elements determination (Table 1). Literature data of three host rock samples from Fengyuan and 36 host rock samples from Nantou are taken from Liao (2003) and Chen et al. (2007) for comparison. The bulk samples from surface outcrops and cores are characterized by high contents of  $\text{SiO}_2$ , and  $\text{Al}_2\text{O}_3$ , and by low concentrations of  $\text{Fe}_2\text{O}_3$ ,  $\text{CaO}$ ,  $\text{K}_2\text{O}$ ,  $\text{MgO}$ ,  $\text{MnO}$ ,  $\text{Na}_2\text{O}$ ,  $\text{P}_2\text{O}_5$ , and  $\text{TiO}_2$  (Fig. 4). The chemical trends in major and minor elements within

the Cholan Formation, the Chinshui Shale, and the Kueichulin Formation are similar to each other. Generally, shales and siltstones usually contain higher  $\text{Al}_2\text{O}_3$ ,  $\text{Fe}_2\text{O}_3$ ,  $\text{MgO}$ ,  $\text{K}_2\text{O}$ , and  $\text{TiO}_2$  and lower  $\text{SiO}_2$  than sandstones because of higher clay contents. The strong positive trends with between  $\text{Al}_2\text{O}_3$  and  $\text{Fe}_2\text{O}_3$ ,  $\text{MgO}$ ,  $\text{K}_2\text{O}$ ,  $\text{TiO}_2$  and strong negative trend between  $\text{Al}_2\text{O}_3$  and  $\text{SiO}_2$  presumably suggest it is mainly mineralogical control on  $\text{Al}_2\text{O}_3$ ,  $\text{Fe}_2\text{O}_3$ ,  $\text{MgO}$ ,  $\text{K}_2\text{O}$ ,  $\text{TiO}_2$  and  $\text{SiO}_2$  contents among three sedimentary formations. However, the strong positive correlations between  $\text{Al}_2\text{O}_3$  and  $\text{Fe}_2\text{O}_3$ ,  $\text{MgO}$ , and  $\text{TiO}_2$ , respectively, also suggest the enrichment of immobile elements Fe, Mg, and Ti take place during chemical weathering. The leaching of the mobile element K is not found; therefore it is suggested that the concentration of K is dominantly controlled by abundance of illite as we mentioned above. Moderate to poor negative trend is also found between  $\text{Al}_2\text{O}_3$  and  $\text{Na}_2\text{O}$  in our samples, suggesting the slight leaching of the mobile element Na during the formation of clay minerals. The great dispersions in the  $\text{Al}_2\text{O}_3$ – $\text{MnO}$  and  $\text{Al}_2\text{O}_3$ – $\text{P}_2\text{O}_5$  diagrams are probably caused by the rarity of  $\text{MnO}$  and  $\text{P}_2\text{O}_5$ .

#### 4.3. Illite chemistry index and illite crystallinity

Wide scatters of illite chemistry index and illite crystallinity are observed in samples from the outcrops and the boreholes. In short,

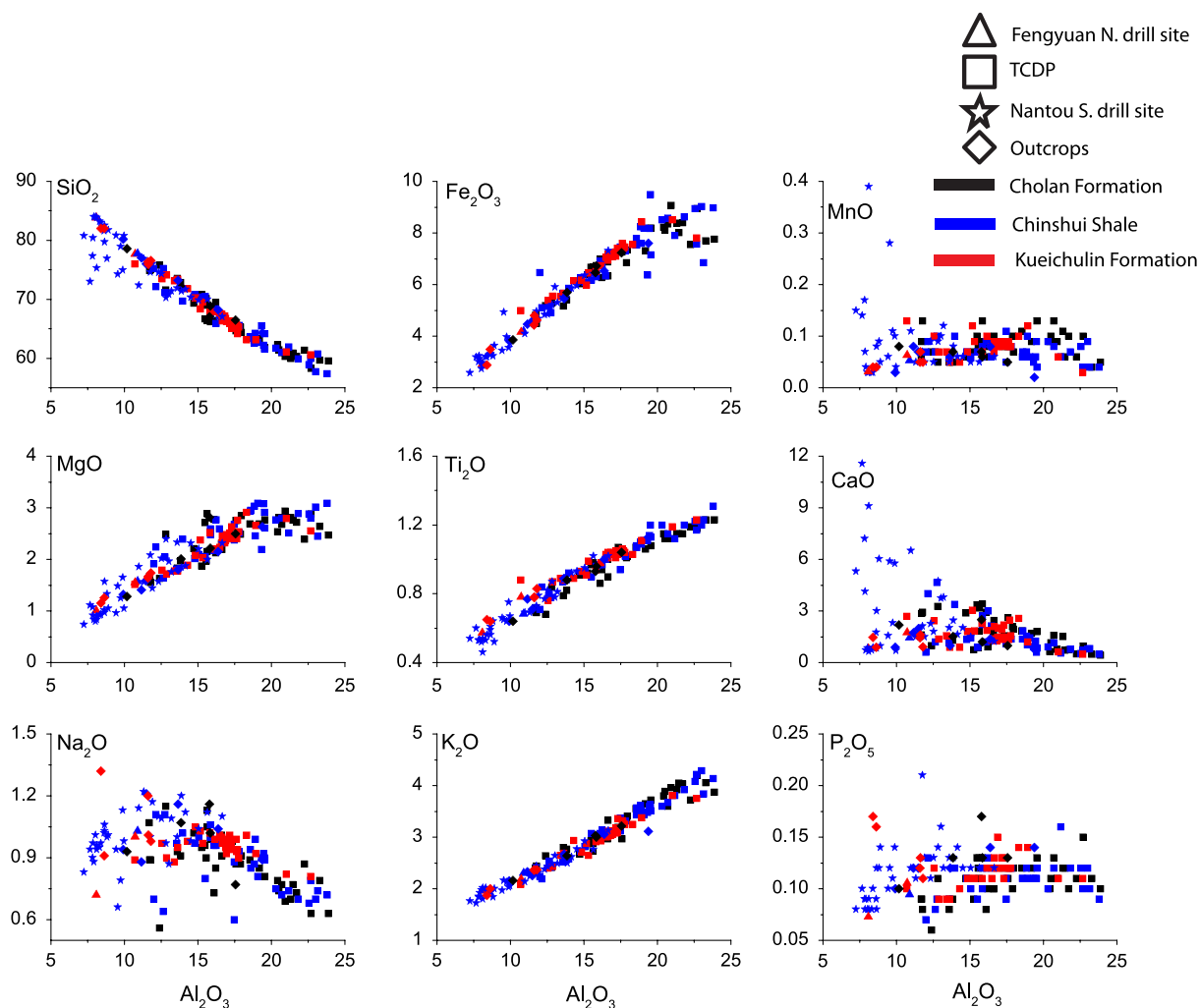


**Fig. 4.** Diagrams of major elements plotted against  $\text{Al}_2\text{O}_3$  in the four outcrops, the two shallow boreholes of Fengyuan and Nantou, and the deep borehole (TCDP). The samples of four outcrops are shown as diamonds. The materials of TCDP site are indicated by squares. The cores of two shallow boreholes of Fengyuan and Nantou are marked as triangles and stars, respectively. Three colors of black, blue, and red are plotted for the Cholan, Chinshui, and Kueichulin Formations, respectively. All patterns are utilized in the following figures. (For interpretation of the references to color in this figure legend, the reader is referred to the web version of this article.)

the average values of illite chemistry index are dispersed from 0.41 to 0.71 in the samples of the outcrops and 0.5–0.65 in the samples of the boreholes (Table 1). The average values of illite crystallinity are distributed from  $0.31^{\circ}\Delta 2\theta$  to  $0.39^{\circ}\Delta 2\theta$  in all locations except the one of TCDP with the lowest value of  $0.25^{\circ}\Delta 2\theta$ . We will combine the data of illite chemistry index and illite crystallinity with mineralogical and chemical proxies and discuss in detail later.

## 5. Discussion

### 5.1. Mineralogical changes

Fresh rocks and minerals are seldom in equilibrium with near-surface waters, temperatures, and pressures (Velde and Meunier, 2008). In the presence of water, rocks and minerals can be chemically modified towards a phase that is more stable in the near-surface environment, e.g., clay minerals. The differences in the clay mineral distributions can be related to weathering, sedimentation, burial, diagenesis, hydrothermal alterations, and tectonic processes (Velde and Meunier, 2008; Vrolijk and van der Pluijm, 1999). In general, the smectite formed by the reaction of the clay fractions in sediments turn transforms as diagenetic processes and yielded illite (e.g., illite–smectite transition observed in the Miocene in the Gulf of Mexico). Whereas, it seems that illite–smectite transition within burial, and diagenetic processes do not result in a dramatic variation on clay mineral assemblages in this study. Moreover, the variety of clay minerals produced by hydrothermal alteration and tectonic processes (fault) can be significant, but is confined to very local areas; whereas, weathering could cause a widespread and high-degree variation in clay minerals (Chamley, 1989; Kuo et al., 2009). To minimize the effect of tectonic processes, we analyzed the host rocks that essentially remained undamaged during faulting. Moreover, to investigate the influences of burial, and diagenesis, relative percentages of illite and smectite of the outcrops, Fengyuan and TCDP versus depth were plotted (Fig. 5). The illite–smectite reaction driven by the processes of burial and diagenesis is not obvious with comparing the

abundance of illite and smectite with depth (Fig. 5). Thus, the significant differences of clay minerals among these materials seem to be due to the weathering.

Generally, weathering is classified as either physical or chemical processes (Weaver, 1989). Physical weathering involves many processes, such as in situ fragmentation, comminution, uploading, thermal expansion, colloidal plucking, and the activity of plants or animals. Illite and chlorite are considered as primary minerals, which reflect low hydrolytic processes in continental weathering and increasing direct rock erosion (Liu et al., 2007, 2009). Considering the maximum depth of burial and correspondingly, temperature, illite and chlorite in our study area presumably have been derived from the erosion of micas and chlorite of metamorphic rocks, mainly derived from the western orogeny belt at high uplift rate (Yue et al., 2005). In contrast, the weathering environment frequently represents a chemical system where pressure is constant, and many chemical elements are mobile and enter the solution from the ambient rocks (Velde and Meunier, 2008). For example, during hydrolysis, subtraction of ions from minerals in parent rocks statistically concerns primarily more mobile ions, like Na, K, Ca, and Mg. This hydrolytic weathering process results in the formation of 2:1 layer clays (the assemblage of two tetrahedral sheets with one octahedral sheet, e.g., smectite) (Pédro, 1981). Transitional elements tend to be depleted later (Mn, Fe), and are followed by Si. This process results in the formation of 1:1 layer clays (the assemblage of one tetrahedral sheet with one octahedral sheet, e.g., kaolinite). Al is the less mobile element through the hydrolytic process. The final process of hydrolytic weathering results in the formation of Al hydroxides (e.g., gibbsite). An increase in chemical weathering intensity and ions subtraction in parent rocks produces secondary minerals that become more and more depleted in cations, especially the more mobile elements.

Based on what we discussed above, two end members of chemical weathering (smectite and kaolinite) and one end member of physical weathering (illite + chlorite) are plotted as ternary diagrams (Fig. 6). It should be noted that smectite-rich samples, which avoid collecting a cm-scale surface weathering reaction from the

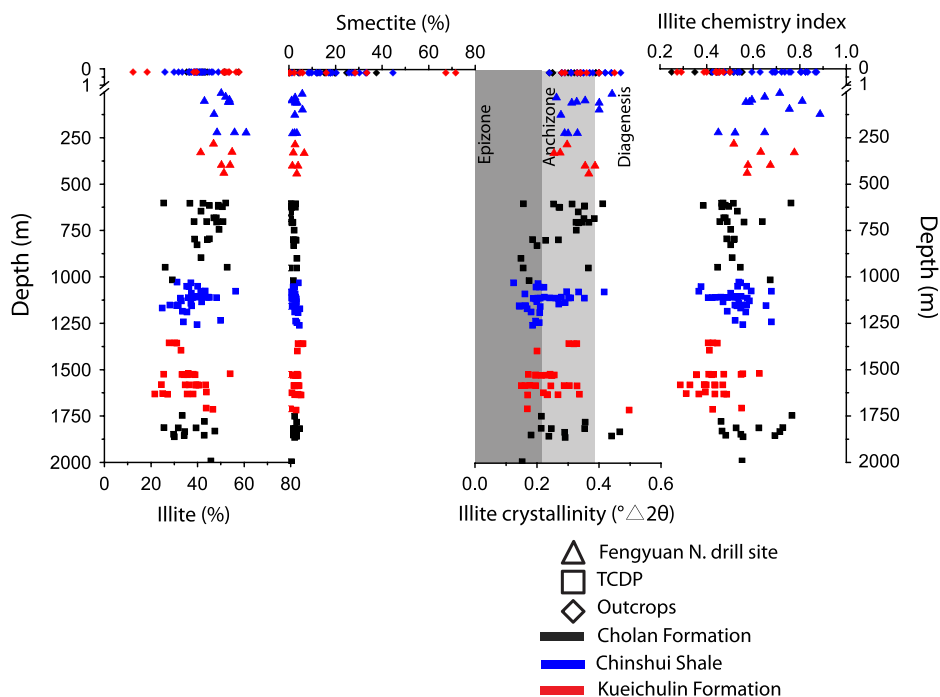
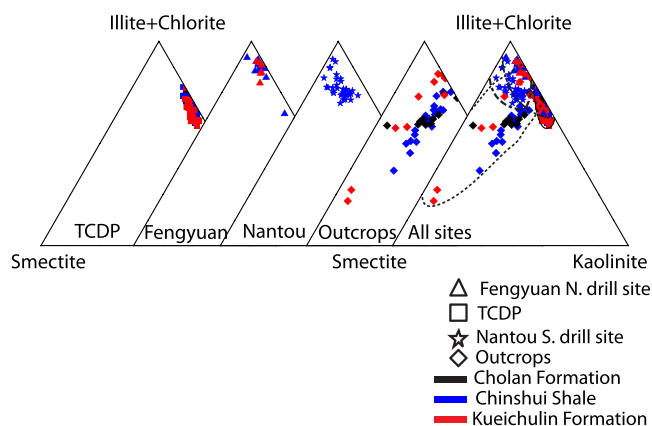


Fig. 5. Variation of illite, smectite, illite chemistry index, and illite crystallinity along depth from boreholes of the four outcrops, Fengyuan and TCDP.



**Fig. 6.** Comparison between clay mineral ternary diagrams of host rocks from the four outcrops, the two shallow boreholes of Fengyuan and Nantou, and the deep borehole (TCDP).

outcrops, skew and widen the weathering rind in Fig. 6. Thus, significantly different distributions of clay mineral assemblages in Fig. 6 were observed from the four surface outcrops, northern and southern boreholes, and TCDP. Micro-observations such as Scanning Electron Microscopy and Transmission Electron Microscopy are probably needed to characterize the occurrence of smectite from the surface to deep depths (Solum et al., 2003) and thus further experiments should be conducted to capture the relevant processes in the future. For the above reason, we conclude that the decreasing abundances of smectite from the surface to deep depth (TCDP) are related to the intensity of chemical weathering. This makes diagenesis as a cause for the decrease in smectite abundance less likely. If such an explanation for the change in smectite abundance is true, the weight percent of smectite along depth in Fig. 5 should gradually become less instead of dramatically decreasing. Thus, the existence of smectite can be used as an indicator for chemical weathering in this study.

**5.2. Mineralogical changes versus illite chemistry index and illite crystallinity**

Assuming presumably that there is no important diagenesis for illite–smectite reaction in our samples, we select illite chemistry index as an indicator for the intensity of chemical weathering (Esquevin, 1969) and illite crystallinity as a proxy for continental sources. Present studies have shown that transition to illite is accompanied by a number of parallel temperature-dependent mineral reactions and crystallographic transformations such as conversion of smectite to mixed-layer smectite/illite to well crystallized illite (muscovite) and increasing illite crystallinity (Hoffman and Hower, 1979; Velde and Meunier, 2008). Thus, the characteristics of illite crystallinity were correlated with metamorphic zones such as anchizone which is exposed under low temperature metamorphism (Kisch, 1980, 1990). The range of anchizone correlated with illite crystallinity was defined in  $0.38^\circ\Delta 2\theta$  to  $0.21^\circ\Delta 2\theta$  by Kisch (1990) and  $0.38^\circ \pm 0.01^\circ\Delta 2\theta$  to  $0.22^\circ \pm 0.01^\circ\Delta 2\theta$  by Chen (1984) and we utilize the value of  $0.38^\circ\Delta 2\theta$  to  $0.21^\circ\Delta 2\theta$  as the range of anchizone in this study (Figs. 5 and 7). Besides, lower values of FWHM of illite also represent higher crystallinity, which is characteristic of weak hydrolysis in continental sources (Chamley, 1989; Krumm and Buggisch, 1991).

To determine the correlation between the illite chemistry index and illite crystallinity with sedimentary formations and/or diagenesis, the illite chemistry index and illite crystallinity versus depth were plotted in Fig. 5. The values of illite chemistry index among

these sedimentary formations are widely distributed and it seems that the distribution of illite chemistry index of the outcrop samples are the widest. The values of illite crystallinity are also widely scattered among the Cholan, Chinsui, and Kueichulin Formations and present a trend that are slightly increasing with decreasing depth (Fig. 5). It is worth pointing out that the reverse trend of illite crystallinity, named “unroofing” by Dorsey et al. (1988) and Buchovecky and Lundberg (1988), is not observed in the profile. This is presumably because of the complex source of sediments including metamorphic lithic-fragments from western Taiwan orogeny and granitic fragments from eastern passive continental edge. Thus, the abundance of clay minerals and mineral assemblages (Fig. 5) are presumably similar in each given formation, the variation of illite chemistry index and illite crystallinity suggests that materials were exposed more severe chemical weathering in the shallow depth.

It seems that the abundance of smectite and the illite chemistry index and illite crystallinity are correlated with the process of chemical weathering. The smectite indicator versus illite chemistry index and illite crystallinity are shown in Fig. 7. The diagrams of illite chemistry index and illite crystallinity show similar patterns, suggesting that the state of physical and chemical weathering could be determined with these three mineralogical parameters in our samples. More than half of the samples from TCDP are observed with low values of illite chemistry index and low values of illite crystallinity, and it suggests that detrital well-crystallized illite might keep the original composition and the crystal structure in depth during physical weathering. On the other hand, most

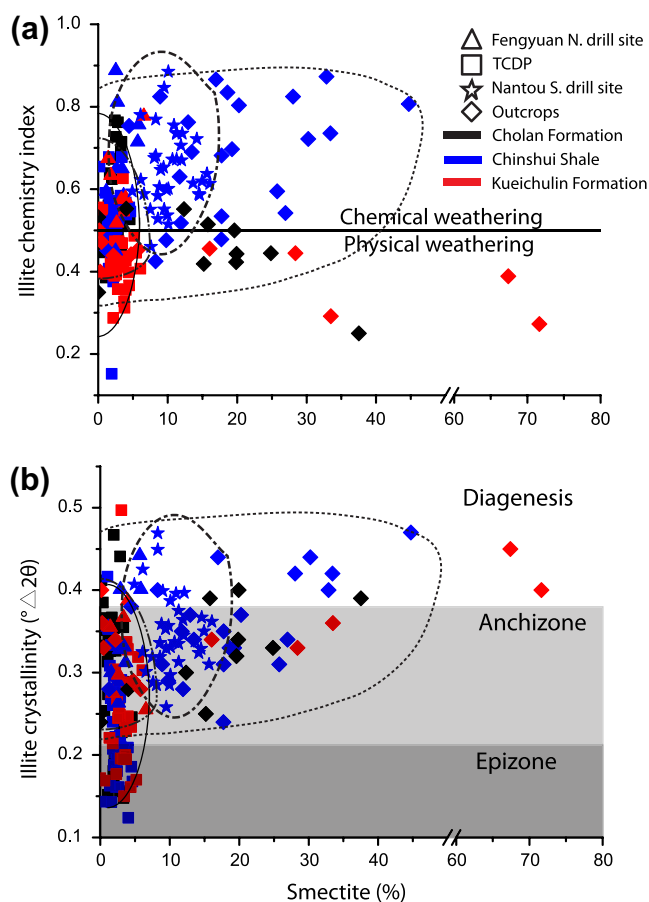


**Fig. 7.** Correlations of relative smectite percentage with (a) illite chemistry index and (b) illite crystallinity in the host rock samples from the four outcrops, the two shallow boreholes of Fengyuan and Nantou, and the deep borehole (TCDP).



samples from the outcrops and the shallow boreholes of Fengyuan and Nantou display high values of illite chemistry index and high values of illite crystallinity. The observation suggests that illite might have been weathered chemically near the surface. It is worth pointing out that the value of illite chemistry index and illite crystallinity is not directly proportional to the relative percentage of smectite. It means that illite converts to illite/smectite mixed-layers by chemical weathering and its composition and crystal structure is not completely changed with the process of solid solution. These results support that the degree of chemical weathering decreases with depth.

### 5.3. Chemical mobility and weathering trends

The major element compositions can be used to assess the state of chemical weathering and to determine their geochemical processes (Vital and Statterger, 2000; Singh et al., 2005; Liu et al., 2007, 2009). The chemical compositions of weathering products are expected to demonstrate a well-established concept on mobility of various elements during weathering (Nesbitt and Young, 1982; Singh et al., 2005; Liu et al., 2007, 2009). Here we use elemental ratios calculated with respect to the least mobile element Al to identify and evaluate the major element mobility. All major elements show similar chemical mobility, albeit with little difference from the surface to the deep depth (Fig. 4). In general, shales with high clay-fraction contains abundant immobile elements, such as Al and Ti, and are depleted in mobile element, especially

in SiO<sub>2</sub>, CaO, K<sub>2</sub>O, Na<sub>2</sub>O, MnO, and MgO. In contrast, the constituents of sandstones are more variable than those of shales, and they may contain high percentage of quartz and other sediments supplying SiO<sub>2</sub> and other minor elements as CaO, K<sub>2</sub>O, Na<sub>2</sub>O, MnO, and MgO (arkoses and greywackes are not included). Thus, the differences of lithology among three sedimentary formations could be used to explain why there is a widespread distribution of all major elements among our study materials. Although the leaching of mobile elements K, Na and Ca, and less mobile element Si, Mn, and Mg during the formation of clay minerals under an intense chemical weathering condition on the surface, for sediments, appears to be true (Liu et al., 2007, 2009), it seems that the solid rocks are not seriously affected by leaching. Thus, the similar trends of chemical mobility with little differences observed in our samples confirm that the Cholan Formation, Chinshui Shale, and Kueichulin Formation have a similar average chemical composition and/or the intensity of chemical weathering from the surface to the deep depth.

The degree of chemical weathering can be estimated by the chemical index of alteration (CIA) defined as:

$$\text{CIA} = [\text{Al}_2\text{O}_3 / (\text{Al}_2\text{O}_3 + \text{CaO}^* + \text{Na}_2\text{O} + \text{K}_2\text{O})] \times 100$$

where CaO\* represents CaO associated with the silicate fraction of the sample (Nesbitt and Young, 1982; Liu et al., 2007, 2009). For example, for primary minerals (non-altered minerals), all feldspars have a CIA value of 50, and the mafic minerals, such as biotite, hornblende, and pyroxenes, have CIA values between of 50–55, 10–30, and 0–10, respectively. Feldspar and mica weathering to smectite

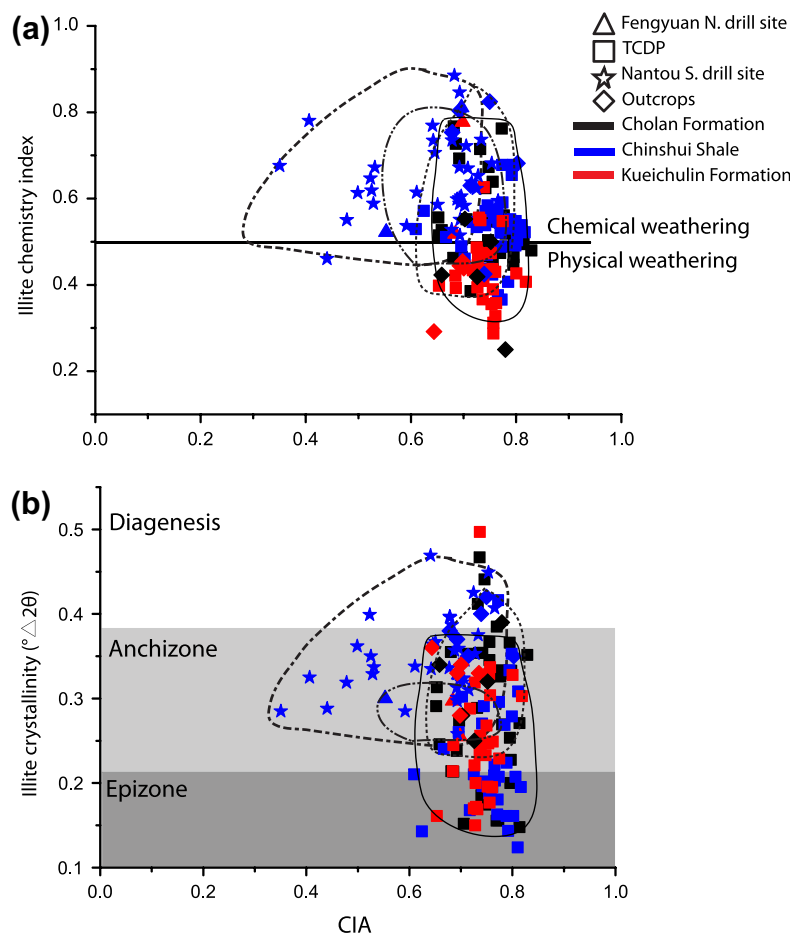


**Fig. 8.** Comparison between chemical index of alteration (CIA) and (a) illite chemistry index and (b) illite crystallinity of host rocks from the four outcrops, the two shallow boreholes of Fengyuan and Nantou, and the deep borehole (TCDP). The graphs show similar correlations of mineralogical and element geochemical proxies of chemical weathering.

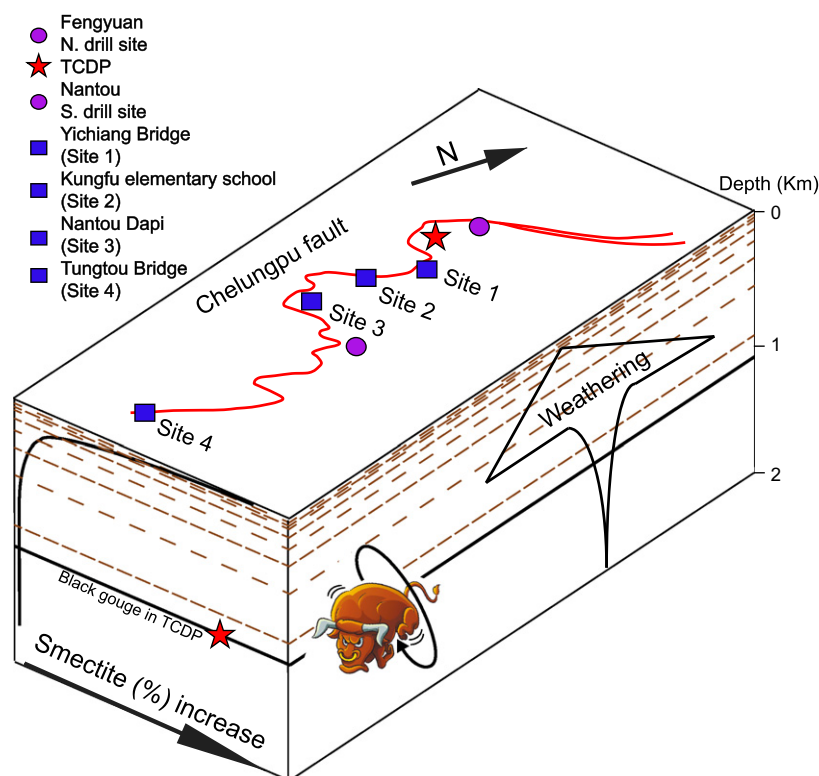


**Fig. 9.** Relative percentage of smectite with depth for host rocks of the four outcrops, the two shallow boreholes of Fengyuan and Nantou, and the deep borehole (TCDP). The variation of the weathering trend is signified along depth. Bull indicates the candidate of principal slip zone of future large earthquake. In China, it was once believed that a giant bull lived underground and caused earthquakes when it turns its own body over.

and kaolinite result in a net loss of K and Na in weathering profiles, whereas Al is resistant and is enriched in weathering products (Nesbitt and Young, 1982). This induces an increase of CIA values to about 100 for kaolinite and 70–85 for smectite. The CIA value is to quantify the chemical weathering of the rocks by considering the loss of labile elements, such as Na, Ca, and K. CIA values are 64–80 for the surface outcrop samples, 55–70 for the northern borehole of Fengyuan samples, 35–77 for the southern borehole of Nantou samples, and 61–83 for the deep borehole of TCDP samples (Fig. 8). Such high CIA values suggest that all samples should have been weathered or altered (Nesbitt and Young, 1982), but it is not in agreement with the mineralogical results on clays (Fig. 6). Moreover, similar grouping of CIA values within different sedimentary formations are obviously observed in the TCDP case (Fig. 8). Therefore, we argue that the high CIA values are controlled by high clay fractions in shales and/or sandstones, instead of the leaching of elements, and this argument is also supported by the major elements (Fig. 4).

The correlation between CIA and the illite chemistry index and crystallinity could be also used to demonstrate the degree of chemical weathering (Liu et al., 2007, 2009; Fig. 8). The values of CIA along with the significantly variable values of illite chemistry index and illite crystallinity among the samples from the surface to the deep depth imply that, for solid rocks, chemical weathering dominantly changes clay mineral structures and/or clay mineral assemblages without loss of major elements.

#### 5.4. Formation of smectite and its implication for faulting mechanism

The formation of smectite in the host rocks is interpreted as the product of chemical weathering which took place near the surface (Fig. 9), and the geochemical data in this study suggest that chemical weathering, rather than leaching of major elements, triggers the phase change of clay minerals. It suggests that the presence

of smectite is neither related to the faulting, nor the weakening of the Chelungpu fault during coseismic events. Therefore, to distinguish the presence of smectite between the host rocks and fault gouges close to the surface is critical, but difficult. This makes the variation of clay minerals a unreliable parameter for understanding the fault behavior unless characteristics of clay mineral phases were exceptionally approached for a fault (e.g., Solum et al., 2003).

Smectite is of extremely low abundance or absent in the TCDP case. Such a low percentage of smectite indicates that smectite should not be responsible for weakening the Chelungpu fault during coseismic events. Whereas, Kuo et al. (2009) examined the characteristics of clay minerals from TCDP, and interpreted that the smectite-rich (devitrified from pseudotachylyte) black gouge (the relative clay percentage of smectite is 85%) as the primary slip zone of the Chelungpu fault (Fig. 9). Ikari et al. (2009) conducted conventional biaxial testing under true-triaxial condition tests with simulated gouge of quartz, illite, chlorite, and montmorillonite (a type of smectite), and provided an extremely low friction coefficient in montmorillonite-rich gouge. On the other hand, conventional triaxial compression test was conducted with binary and ternary mixtures of quartz, montmorillonite (a type of smectite), and illite and the trend was a decrease in strength with increasing smectite content (Tembe et al., 2010). Thus, although smectite may not play important role in the past coseismic events, the presence of smectite-rich black gouge of the Chelungpu fault, in the TCDP case, might be relatively critical which is a possible candidate to trigger the Chelungpu fault for future seismic events.

## 6. Conclusion

The clay mineralogical and geochemistry results from this study of the Chelungpu fault demonstrate that the degree of chemical weathering in the host rocks varies depth. Clay mineralogical indicators (the relatively percentage of smectite, illite chemistry index,

and illite crystallinity) and major elemental indexes (chemical mobility, CIA index), indicate that the intensity of chemical weathering decreases from the surface to the deep borehole in TCDP. For the solid host rocks, chemical weathering makes rocks and minerals transform towards smectite, which is more stable in the near-surface environment, without severely leaching the major elements. Therefore, the presence of smectite in the outcrops may not play a significant role during faulting, and the clay mineralogical data suggest that fault-weakening mechanism within smectite cannot be applied to the Chelungpu fault during coseismic events.

## Acknowledgements

We thank the working group of TCDP, including the drilling company Fang-Yu and Wan-Da, the on-site assistants and participating students from NTU and NCU. The research was supported by the National Science Council, Republic of China, under Grants of NSC 97-2627-M-002-007, and 98-2627-M-002-002, and National Natural Science Foundation of China (41102135).

## References

- Biscaye, P.E., 1965. Mineralogy and sedimentation of recent deep-sea clays in the Atlantic Ocean and adjacent seas and oceans. *Geological Society of American Bulletin* 76, 803–832.
- Boutareaud, S., Boullier, A.M., Andreani, M., Calugaru, D.G., Beck, P., Song, S.R., Shimamoto, T., 2010. Clay clast aggregates in gouges: new textural evidence for seismic faulting. *Journal of Geophysical Research* 115, B02408, doi: 10.1029/2008JB006254.
- Brantut, N., Schubnel, A., Rouzaud, J.-N., Brunet, F., Shimamoto, T., 2008. High-velocity frictional properties of a clay-bearing fault gouge and implications for earthquake mechanics. *Journal of Geophysical Research* 113, B10401. <http://dx.doi.org/10.1029/2007JB005551>.
- Buchovecky, E.J., Lundberg, N., 1988. Clay mineralogy of mudstone from the southern Coastal Range: unroofing of the orogen versus in-situ diagenesis. *Acta Geologica Taiwanica* 26, 247–261.
- Byerlee, J.D., 1970. The mechanics of stick slip. *Tectonophysics* 9 (5), 475–486.
- Chamley, H., 1989. *Clay Sedimentology*. Springer, New York, p. 623.
- Chen, C.H., 1984. Determination of lower greenschist facies boundary by K-mica-chlorite crystallinity in the Central Range of Taiwan. *Geological Society of China Proceedings* 27, 41–53.
- Chen, Y.G., Chen, W.S., Lee, J.C., Lee, Y.H., Lee, C.T., Chang, H.C., Lo, H.C., 2001. Surface rupture of 1999 Chi-Chi earthquake yields insights on active tectonics of central Taiwan. *Bulletin of Seismological Society of America* 91, 977–985.
- Chen, W.M., Tanaka, H., Huang, H.J., Lu, C.B., Lee, C.Y., Wang, C.Y., 2007. Fluid infiltration associated with seismic faulting: examining chemical and mineralogical composition of fault rocks from the active Chelungpu fault. *Tectonophysics* 443, 243–254.
- Chiu, H.T., 1971. Folds in the northern half of western Taiwan. *Petroleum Geology of Taiwan* 8, 7–19.
- Covey, M., 1984. Lithofacies analysis and basin reconstruction, Plio-Pleistocene Western Taiwan foredeep. *Petrological Geology of Taiwan* 20, 53–83.
- Di Toro, G., Han, R., Hirose, T., De Paola, N., Nielsen, S., Mizoguchi, K., Ferri, F., Cocco, M., Shimamoto, T., 2011. Fault lubrication during earthquakes. *Nature* 471. <http://dx.doi.org/10.1038/nature09838>.
- Dorsey, R.J., Buchovecky, E.J., Lundberg, N., 1988. Clay mineralogy of Pliocene–Pleistocene mudstones, eastern Taiwan: Combined effects of burialdiagenesis and provenance unroofing. *Geology* 16, 944–947.
- Esquevin, J., 1969. Influence de la composition chimique des illites sur leur cristallinité. *Bulletin de Centre Rech. Pau SNPA* 3, 147–153.
- Fagel, N., Boski, T., Likhoshway, L., Oberhaensli, H., 2003. Late quaternary clay mineral record in central lake Baikal (Academician Ridge, Siberia). *Palaeogeography, Palaeoclimatology, Palaeoecology* 193, 159–179.
- Faulkner, D.R., Rutter, E.H., 2001. Can the maintenance of overpressured fluids in large strike-slip fault zones explain their apparent weakness? *Geology* 29, 503–506.
- Gingeles, F.X., 1996. Holocene climatic optimum in Southwest Africa—evidence from the marine clay mineral record. *Palaeogeography, Palaeoclimatology, Palaeoecology* 122, 77–87.
- Gingeles, F.X., De Deckker, P., Hillenbrand, C.-D., 2001. Clay mineral distribution in surface sediments between Indonesia and NW Australia—source and transport by ocean current. *Marine Geology* 179, 135–146.
- Han, R., Shimamoto, T., Hirose, T., Ree, J.-H., Ando, J.-I., 2007. Ultralow friction of carbonate faults caused by thermal decomposition. *Science* 316, 878. <http://dx.doi.org/10.1126/science.1139763>.
- Heermance, R.V., 2002. Geometry and Physical Properties of the Chelungpu Fault, Taiwan, and their Effect on Fault Rupture. Master Thesis, Utah State University, Logan, Utah, USA.
- Heermance, R.V., Shipton, Z.K., Evans, J.P., 2003. Fault structure control on fault slip and ground motion during the 1999 rupture of the Chelungpu fault, Taiwan. *Bulletin of Seismological Society of America* 93, 1034–1050.
- Hirono, T., Fujimoto, K., Yokoyama, T., Hamada, Y., Tanikawa, W., Tadaï, O., Mishima, T., Tanimizu, M., Lin, W., Soh, W., Song, S.R., 2008. Clay mineral reactions caused by frictional heating during an earthquake: an example from the Taiwan Chelungpu fault. *Geophysical Research Letters* 35, L16303. <http://dx.doi.org/10.1029/2008GL034476>.
- Ho, C.S., 1988. An Introduction to the Geology of Taiwan—Explanatory Text of the Geologic Map of Taiwan, second ed., Central Geological Survey, MOEA, Taipei, Taiwan, ROC, p. 163.
- Hoffman, J., Hower, J., 1979. Clay mineral assemblages as low-grade metamorphic geothermometers: application to the thrust-faulted, disturbed belt of Montana, USA. In: Scholle, P.A., Schluger, P.R. (Eds.), *Aspects of diagenesis*. Society of Economic Paleontologists and Mineralogists Special Publication, vol. 26, pp. 55–79.
- Ikari, M.J., Saffer, D.M., Marone, C., 2009. Frictional and hydrologic properties of clay-rich fault gouge. *Journal of Geophysical Research* 114, B05409. <http://dx.doi.org/10.1029/2008JB006089>.
- Isaacs, A.J., Evans, J.P., Song, S.R., Kolesar, P.T., 2007. Characterizing brittle deformation, damage parameters, and clay composition in fault zones: variations along strike and with depth in the Chelungpu Fault zone. *Terrestrial Atmospheric and Oceanic Science* 18, 183–221.
- Jones, R.M., Hillis, R.R., 2003. An integrated, quantitative approach to assessing fault-seal risk. *American Association of Petroleum Geologists Bulletin* 87, 507–524.
- Kahle, M., Kleber, M., Jahn, R., 2002. Review of XRD-based quantitative analyses of clay minerals in soils: the suitability of mineral intensity factors. *Geoderma* 109, 191–205.
- Kao, H., Chen, W., 2000. The Chi-Chi earthquake sequence; active, out-of-sequence thrust faulting in Taiwan. *Science* 228, 2346–2349.
- Kisch, H.J., 1980. Coal rank and illite crystallinity associated with the zeolite facies of southland and the pumpellyite-bearing facies of Otago, southern New Zealand. *New Zealand Journal of Geological Geophysics* 24 (3), 349–360.
- Kisch, H.J., 1990. Calibration of the anchizone: a critical comparison of illite “crystallinity” scales used for definition. *Journal of Metamorphic Geology* 8, 31–46.
- Kisch, H.J., 1991. Illite crystallinity: recommendations on sample preparation, X-ray diffraction settings, and interlaboratory samples. *Journal of Metamorphic Geology* 9, 665–670.
- Krumm, S., Buggisch, W., 1991. Sample preparation effects on illite crystallinity measurements: grain size gradation and particle orientation. *Journal of Metamorphic Geology* 9, 671–677.
- Kübler, B., 1964. Les argiles, indicateurs de métamorphisme. *Revue de L'Institut Français du Pétrole* 19, 1093–1112.
- Kübler, B., 1967. La cristallinité de l'illite et les zones tout à fait supérieures du métamorphisme. In: *Étages Tectoniques. Colloque de Neuchâtel 1966*, pp. 105–121.
- Kuo, L.W., Song, S.R., Yeh, E.C., Chen, H.F., 2009. Clay mineral anomalies in the fault zone of Chelungpu Fault, Taiwan, and its implication. *Geophysical Research Letters* 36, L18306. <http://dx.doi.org/10.1029/2009GL039269>.
- Kuo, L.W., Song, S.R., Huang, L., Yeh, E.C., Chen, H.F., 2011. Temperature estimates of coseismic heating in clay-rich fault gouges, the Chelungpu fault zone, Taiwan. *Tectonophysics* 502, 315–327.
- Lee, J.C., Chen, Y.G., Sieh, K., Mueller, K., Chen, W.S., Chu, H.T., Chan, Y.C., Rubin, C., Yates, R., 2001. A vertical exposure of the 1999 surface rupture of the Chelungpu fault at Wufeng, western Taiwan: structural and paleoseismic implications for an active thrust fault. *Bulletin of Seismological Society of America* 91 (5), 914–929.
- Liao, C.F., 2003. Analysis of Fault Rock Deformation and Clay Minerals from Fault Cores of Chelungpu Fault zone. Master's Thesis of National Central University, p. 132 (in Chinese, summary in English).
- Lin, M.L., Cheng, F.S., Weng, T.H., Hung, J.C., Li, C.Y., Chou, Y.H., Chu, L.Y., Li, C.N., Huang, W.C., Kao, C.S., 2000. The Research of Rock Mechanics of the Fault Gouge. Report of Ministry of Transportation and Communications of Taiwan area National Expressway Engineering Bureau, pp. 90–95 (in Chinese).
- Lin, A., Ouchi, T., Chen, A., Maruyama, T., 2001. Co-seismic displacements, folding and shortening structures along the Chelungpu surface rupture zone occurred during the 1999 Chi-Chi, Taiwan earthquake. *Tectonophysics* 330, 225–244.
- Liu, Z., Colin, C., Huang, W., Le, K.P., Tong, S., Chen, Z., Trentesaux, A., 2007. Climatic and tectonic controls on weathering in South China and the Indochina Peninsula: clay mineralogical and geochemical investigations from the Pearl, Red, and Mekong drainage basins. *Geochemistry, Geophysics, Geosystems* 8, Q05005. <http://dx.doi.org/10.1029/2006GC001490>.
- Liu, Z., Zhao, Y., Colin, C., Siringan, F.P., Wu, Q., 2009. Chemical weathering in Luzon, Philippines from clay mineralogy and major-element geochemistry of river sediments. *Applied Geochemistry* 24, 2195–2205. <http://dx.doi.org/10.1016/j.apgeochem.2009.09.025>.
- Lockner, D.A., Morrow, C., Moore, D., Hickman, S., 2011. Low strength of deep San Andreas fault gouge from SAFOD core. *Nature* 472, 82–86.
- Ma, K.F., Song, T.R.A., Lee, S.J., Wu, H.L., 2000. Spatial slip distribution of the September 20, 1999, Chi-Chi, Taiwan, earthquake,  $M_w$  7.6 – inverted from teleseismic data. *Geophysical Research Letters* 27, 3417–3420.
- Meunier, A., Velde, B., 2004. Illite. Springer, p. 140.

- Mizoguchi, K., Hirose, T., Shimamoto, T., Fukuyama, E., 2009. High-velocity frictional behavior and microstructures evolution of fault gouge obtained from Nojima fault, southwest Japan. *Tectonophysics* 471, 285–296.
- Moore, D.M., Reynolds Jr., R.C., 1997. *Individual Clay Minerals, X-ray Diffraction and the Identification and Analysis of Clay Minerals*. Oxford University Press, New York (Chapter 5).
- Mount, V., Suppe, J., 1987. State of stress near the San Andreas fault: implications for wrench tectonics. *Geology* 15, 1143–1146.
- Nesbitt, H.W., Young, G.M., 1982. Early Proterozoic climates and plate motions inferred from major element chemistry of lutites. *Nature* 299, 715–717.
- Pédro, G., 1981. Les grands traits de l'évolution cristallogénétique des minéraux au cours de l'altération superficielle des roches. *Rend. Society Italy Mineralogical Petrology* 37, 633–666.
- Rice, J.R., 1992. Fault stress states, pore pressure distributions, and the weakness of the San Andreas Fault. In: Evans, B., Wong, T.-f. (Eds.), *Fault Mechanics and Transport Properties of Rocks; A Festschrift in Honor of W. F. Brace*. Academic Press, San Diego, pp. 475–503.
- Sibson, R.H., 1990. Conditions for fault-valve behaviour. In: Knipe, R.J., Rutter, E.H. (Eds.), *Deformation Mechanisms, Rheology and Tectonics*. Geological Society Special Publication, vol. 54, pp. 15–28.
- Sibson, R.H., 2003. Brittle-failure controls on maximum sustainable overpressure in different tectonic regimes. *AAPG Bulletin* 87, 901–908.
- Singh, M., Sharma, M., Tobschall, H.J., 2005. Weathering of the Ganga alluvial plain, northern India: implications from fluvial geochemistry of the Gomati River. *Applied Geochemistry* 20, 1–21.
- Solum, J.G., van der Pluijm, B.A., Peacor, D.R., 2003. Influence of phyllosilicate mineral assemblages, fabrics, and fluids on the behavior of the Punchbowl fault, southern California. *Journal of Geophysical Research* 108 (B5), 2233.
- Solum, J.G., van der Pluijm, B.A., Peacor, D.R., 2005. Neocrystallization, fabrics and age of clay minerals from an exposure of the Moab fault, Utah. *Journal of Structural Geology* 27, 1563–1576.
- Suppe, J., 1981. Mechanics of mountain building and metamorphism in Taiwan. *Memoir of the Geological Society of China* 4, 67–89.
- Takahashi, M., Mizoguchi, K., Kitamura, K., Masuda, K., 2007. Effects of clay content on the frictional strength and fluid transport property of faults. *Journal of Geophysical Research* 112, B08206.
- Tanaka, H., Wang, C.Y., Chen, W.M., Sakaguchi, A., Ujie, K., Ito, H., Ando, M., 2002. Initial science report of shallow drilling penetrating into the Chelungpu fault zone, Taiwan. *Terrestrial Atmospheric and Oceanic Science* 13, 227–251.
- Tembe, S., Lockner, D.A., Wong, T.F., 2010. Effect of clay content and mineralogy on frictional sliding behavior of simulated gouges: binary and ternary mixtures of quartz, illite, and montmorillonite. *Journal of Geophysical Research* 115, B03416. <http://dx.doi.org/10.1029/2009JB006383>.
- Velde, B., Meunier, A., 2008. *The Origin of Clay Minerals in Soils and Weathered Rocks*. Springer, p. 13.
- Vital, H., Stettger, K., 2000. Major and trace elements of stream sediments from the lowermost Amazon River. *Chemical Geology* 168, 151–168.
- Vrolijk, P., van der Pluijm, B.A., 1999. Clay gouge. *Journal of Structural Geology* 21, 1039–1048.
- Wan, S., Li, A., Clift, P.D., Wu, S., Xu, K., Li, T., 2010. Increased contribution of terrigenous supply from Taiwan to the northern South China Sea since 3Ma. *Marine Geology* 278, 115–121.
- Wang, C.-Y., 1984. On the constitution of the San Andreas fault zone in central California. *Journal of Geophysical Research* 89, 5858–5866.
- Weaver, C.E., 1989. *Developments in Sedimentology 44 – Clays, Muds, and Shales*. Elsevier, New York.
- Whitney, G., 1990. Role of water in the smectite-to-illite reaction. *Clays and Clay Minerals* 38 (4), 343–350.
- Yang, T.Y., Yang, C.C., Lee, C.Y., Chung, S.L., Chen, C.H., 1996. NTUG rock standards for geochemical analysis. *Journal of the Geological society of China* 39 (3), 307–323.
- Yielding, G., Freeman, B., Needham, D.T., 1997. Quantitative fault seal prediction. *American Association of Petroleum Geologists Bulletin* 81, 897–917.
- Yue, L.F., Suppe, J., Hung, J.H., 2005. Structural geology of a classic thrust belt earthquake: the 1999 Chi-Chi earthquake Taiwan (Mw = 7.6). *Journal of Structural Geology* 27, 2058–2083.
- Zoback, M.D., 2000. Strength of the San Andreas Fault. *Nature* 405, 31–32.